Blood glucose control contributes to protein stability of Ski-related novel protein N in a rat model of diabetes

LUQUN LIANG[1,2*], SHUANG LI[1-3*], HUIMING LIU[1,2], YANWEN MAO[1,2], LINGLING LIU[1,2], XIAOHUAN ZHANG[1,2], WEI PENG[1,2], YING XIAO[1,2], FAN ZHANG[2,4], MINGJUN SHI[2,4], YUANYUAN WANG[1,2] and BING GUO[2,4]

[1]State Key Laboratory of Functions and Applications of Medicinal Plants; [2]Department of Pathophysiology, Guizhou Medical University, Guiyang, Guizhou 550025; [3]Department of Pathology, Guizhou Provincial People's Hospital, Guiyang, Guizhou 550002; [4]Guizhou Provincial Key Laboratory of Pathogenesis and Drug Research on Common Chronic Diseases, Guizhou Medical University, Guiyang, Guizhou 550025, P.R. China

Received July 3, 2019; Accepted June 30, 2021

DOI: 10.3892/etm.2021.10776

Abstract. Ski-related novel protein N (SnoN) negatively regulates the transforming growth factor-β1 (TGF-β1)/Smads signaling pathway and is present at a low level during diabetic nephropathy (DN), but its underlying regulatory mechanism is currently unknown. The present study aimed to assess the effects of insulin-controlled blood glucose on renal SnoN expression and fibrosis in rats with diabetes mellitus (DM). Streptozotocin-induced DM rats were treated with insulin glargine (INS group) following successful model establishment. Blood samples were collected and centrifuged for biochemical indexes and the kidneys were collected for morphological analysis. *In vitro*, rat renal proximal tubular epithelial cells were treated with high-glucose medium for 24 h and transferred to normal glucose medium for 24 h. The expression levels of TGF-β1, SnoN, Smad ubiquitin regulatory factor 2 (Smurf2), Arkadia, Smads, E-cadherin, α-smooth muscle actin and collagen III were assessed by western blotting and immunohistochemistry. The ubiquitylation of SnoN was detected by immunoprecipitation, and the expression levels of SnoN mRNA were evaluated by reverse transcription-quantitative PCR. The biochemical parameters and morphology indicated that renal fibrosis was notable in the DM group and mitigated in the INS group. Compared with the control group, TGF-β1, phosphor (p)-Smad2, p-Smad3, Smurf2 and Arkadia levels were enhanced in the DM group, and the levels of SnoN protein were decreased, whereas the levels of SnoN mRNA and ubiquitylation were increased in renal tissues. Notably, treatment with insulin reversed this trend. Furthermore, changing the glucose levels in the medium from high to normal glucose suppressed the epithelial-mesenchymal transition of NRK-52E cells by restoring the SnoN protein levels, and this phenomenon was impaired by the knockout of SnoN. SnoN protein levels were likely reduced through a mechanism enhanced by the ubiquitin proteasome system, which reversed the transcriptional activation of SnoN during DN progression. In addition, controlling blood glucose may delay DN fibrosis by rescuing the protein stability of SnoN.

Correspondence to: Dr Yuanyuan Wang or Professor Bing Guo, Department of Pathophysiology, Guizhou Medical University, Wuben Building C412, Dongqing Road, Guiyang, Guizhou 550025, P.R. China
E-mail: yuan.yuan.wang@outlook.com
E-mail: guobingbs@126.com

*Contributed equally

Key words: diabetic nephropathy, transforming growth factor-β1, Ski-related novel protein N, ubiquitination, Smad ubiquitin regulatory factor 2, Arkadia

Introduction

Diabetic nephropathy (DN) is one of the most serious complications of diabetes mellitus (DM) (1). According to the International Diabetes Federation, there were 370 million patients with DM worldwide in 2011; this number is estimated to reach 550 million in 2030 (2). With the increasing incidence of DM, DN has become one of the major causes of chronic renal failure; ~24.8% of renal failure cases are caused by DN (3). DN can induce lesions in the glomerulus and renal tubules, which eventually cause glomerulosclerosis and tubular fibrosis (4).

The cytokine transforming growth factor-β1 (TGF-β1) exerts a strong effect on fibrosis; the Smad signaling pathway is considered to be the main signal transduction pathway of TGF-β1, and the activation of this pathway serves an important role in the pathogenesis of DN (5). Under high-glucose conditions, a variety of kidney cells secrete TGF-β1, which binds to the TGF-βII receptor (Tβ RII), activating TGF-βI receptor (Tβ RI) kinase, leading to the phosphorylation of Smad2 and Smad3 proteins and the formation of a protein complex with Smad4 (6,7). This activation results in changes of the inherent phenotype of renal cells that promote the accumulation of extracellular matrix (ECM), which serves a key role in the development of tubulointerstitial fibrosis (6). Previous studies have demonstrated that the transcriptional

co-inhibition factor Ski-related novel protein N (SnoN) antagonizes the fibrosis induced by the TGF-β1/Smads signaling pathway (7,8). The inhibition of SnoN promotes renal fibrosis, and the restoration of SnoN expression reduces or delays the development of renal fibrosis (9,10), which suggests that the decrease in the SnoN protein levels is involved in the incidence and development of renal fibrosis.

Since cytoplasmic SnoN exerts a biological effect of a 'switch' in the TGF-β1/Smads signaling pathway, the expression of this protein is tightly regulated by TGF-β1 in terms of both transcriptional activation and protein stability (11). TGF-β1 upregulates SnoN transcription in cancer cells and kidney tissue of rats with unilateral ureteral obstruction (12,13). Other studies have demonstrated that TGF-β1 rapidly and significantly reduces the expression of SnoN protein through specific recognition of the E3 ubiquitin enzymes Arkadia and Smad ubiquitin regulatory factor 2 (Smurf2), which enhances the ubiquitin-mediated degradation of SnoN via activated Smads (13,14). Furthermore, SnoN protein levels during the development of DN are caused by a defect in protein stability mediated by TGF-β-activated kinase 1 (TAK1) (15). TAK1 mediates the phosphorylation of SnoN, resulting in SnoN ubiquitination and eventual degradation, which enhances the epithelial-mesenchymal transition (EMT) and ECM deposition to promote renal fibrosis during DN (15,16). Controlling blood glucose may inhibit the development of DN (17,18). However, further studies are needed to characterize the association between blood glucose control and renal injury in DM rats and to determine whether SnoN is a target for delaying and reversing DN lesions. The present study aimed to examine the effects of insulin-controlled blood glucose on DN fibrosis development and the expression levels of Smurf2, Arkadia and SnoN in renal tissues. The present study investigated changes of SnoN in DN fibrosis, which may provide a theoretical basis for clinical treatment of DN with novel effective targets.

Materials and methods

Experimental animals. Male Sprague-Dawley rats (weight, 160-200 g; age, 6-8 weeks) were purchased from Beijing Fukang Biotechnology Co. Ltd. [license no. SCXK (Jing) 2009-0004] and maintained in the animal center of Guizhou Medical University (Guizhou, China). The rats were housed in a room with a stable ambient temperature of 18-22˚C in wire cages with free access to a standard diet and tap water. The study was conducted in accordance with the guidelines of the National Health and Medical Research Council of China's code for the care and use of animals for scientific purposes and was approved by the Animal Experimental Ethical Inspection Form of Guizhou Medical University (approval no. 1503092). The blood glucose levels were measured in all rats prior to the start of the experiment using a glucometer (Johnson & Johnson). The rats were randomly allocated into three groups (n=6 rats/group): i) Normal control (NC); ii) diabetes mellitus (DM); and iii) insulin treatment (INS). The DM model was established by tail-vein administration of 55 mg/kg streptozotocin (STZ; MilliporeSigma). STZ was dissolved in 0.1 M citrate buffer (pH 4.5). The NC group received the same volume of the vehicle. On day 3 post-STZ injection, fasting glycemic measurements were performed on blood samples (20-50 μl) from the tail vein, and animals with blood glucose levels ≥16.7 mmol/l for ≥3 days were considered diabetic.

Anesthesia and euthanasia. The use of ether was approved by the ethics committee. For anesthesia, the rats were placed into a glass jar with a small beaker containing a cotton ball soaked with 10 ml ether and observed. When the tension of the limbs of the animal was reduced and the corneal reflex was dull, the onset of anesthesia was confirmed. During the course of the experiment, the changes in the depth of anesthesia were observed and, if necessary, the ether beaker was placed on the nose of the animals to maintain the anesthesia. Under anesthesia, blood was drawn from the femoral artery, and the rats were sacrificed by cervical dislocation.

Experimental protocol. Diabetic rats were randomly divided into two groups. For the DM group, diabetes was induced and lasted for 16 weeks. For the INS group, at 12 weeks post-diagnosis, insulin glargine (8-16 U/kg; Sanofi) was injected daily for 4 weeks to maintain blood glucose <10 mmol/l. The NC and DM groups received daily injections of equivalent volumes of citrate buffer. Blood samples were obtained from the tail vein. During insulin treatment, blood glucose levels were measured twice daily, and body weights were obtained weekly.

After completing the treatment, 24-h urine of each rat was collected, the total urine volume was recorded, and the rats were sacrificed. The urine volume was measured, and 24-h urine protein was tested with a Beckman 1650 automated biochemical analyzer (Beckman Coulter, Inc.). Urine protein excretion (mg/24 h) was assessed as urine protein (mg/ml) x urine volume (ml)/24 h. Additionally, tail vein blood was collected to assess the glycosylated hemoglobin A1 (HbA1c) levels.

At the end of the study, the rats were sacrificed under anesthesia following a 6 h fasting period. The serum was prepared by centrifugation (2,750 x g; 15 min, 4˚C) from the femoral artery for the detection of blood glucose. The kidneys of rats were collected; one kidney from each rat was preserved at -80˚C for western blot analysis and reverse transcription-quantitative (RT-q)PCR, whereas the other was fixed with 4% paraformaldehyde (24 h; room temperature) for histological and immunohistochemical evaluation.

H&E staining. The paraffin-embedded kidney sections (3 μm) were baked in the oven at 60˚C for 1 h, placed in two cylinders of xylene successively, each for 10 min, then placed in 100, 100, 95, 95, 95 and 80% ethanol for 5 min each, washed with distilled water for 5 min and then stained with 0.5% hematoxylin for 1-2 min (room temperature). After soaking in water for 15 min, sections were dyed with 1% eosin for 2-5 min (room temperature) and washed with water. The samples were dehydrated with 80, 95, 95, 100 and 100% ethanol for 2 sec each, then passed through xylene I and xylene II for 2 min each. The samples were sealed with neutral gum and observed under the light microscope (magnification, x200 and x400; 8 samples/group; 10 randomly selected fields of view/sample).

Masson staining. Paraffin-embedded renal sections were prepared as aforementioned. Sections were stained with 0.5% hematoxylin for 4-5 min (room temperature) and washed

with water for 2 min. Sections underwent 0.5% hydrochloric acid alcohol differentiation for 10-30 sec at room temperature before being washed with water for 5 min and stained with Masson complex staining solution for 4-5 min (room temperature). After washing with 0.2% acetic acid solution, 5% phosphomolybdic acid solution was added (room temperature) for 5-10 min, followed by further washing with 0.2% acetic acid solution. Sections were exposed to 2% aniline blue solution for 10-30 sec (room temperature), washed with absolute ethanol and allowed to dry. The samples were sealed with neutral gum and observed under the light microscope (magnification, x200 and x400; 8 samples/group; 10 randomly selected fields of view/sample).

Immunohistochemical staining. Paraffin-embedded renal sections (thickness, 4 μm) were baked in the oven at 60˚C for 1 h and placed into three cylinders of xylene successively (10 min each), followed by 100, 100, 95, 90, 80 and 70% ethanol for 5 min each. After washing with ddH_2O for 5 min, 3% H_2O_2, was added at room temperature in dark for 10 min before washing with ddH_2O for 5 min. Antigen repair was performed using a microwave (100˚C, 3 times, 7 min each). After cooling, each piece was sealed with 5% bovine serum albumin (Beijing Solarbio Science & Technology Co., Ltd.) at room temperature for 1 h. The sections were incubated with rabbit collagen (Col)-III primary antibody (1:100; ProteinTech Group, Inc.; cat. no. 22734-1-AP) overnight at 4˚C. The sections were rewarmed for 30 min (room temperature) and washed 3 times with TBST (0.08% Tween-20) for 5 min each. Corresponding biotinylated secondary antibody (1:100; Beijing Zhongshan Jinqiao Biotechnology; cat. no. PV-6001) was added at room temperature for 1 h. Following washing for 10 min with TBST (three times), Avidin/Biotinylated HRP complex was added at room temperature for 30 min and sections were washed with ddH_2O for 5 min. DAB was used to develop color (5 min; room temperature). After washing with ddH_2O for 5 min, 0.5% hematoxylin was added for 1-5 min (room temperature). After washing with water, sections were dehydrated using a gradient of 70, 80, 90, 95 and 100% ethanol for 5 min each. After soaking in xylene three times (1 min each), samples were sealed with neutral gum and observed under the light microscope (magnification, x200 and x400; 8 samples/group; 10 randomly selected fields of view/sample).

Immunofluorescence. The renal tissue was frozen and fixed with 3.7% paraformaldehyde at room temperature for 10 min. Following blocking with 10% donkey serum (Jackson ImmunoResearch Labor atories, Inc.) for 1 h at room temperature), the samples were incubated overnight with antibodies against E-cadherin (1:50; cat. no. 20874-1-AP; ProteinTech Group, Inc.) at 4˚C. E-cadherin expression was detected with Cy3-conjugated goat anti-mouse secondary antibodies (room temperature, 1 h; 1:50; cat. no. PMK-014-096S; Wuhan Pomeike Biotechnology Co., Ltd.). DAPI was used as a counterstain, and fluorescence was detected under a Leica DM4000B microscope Leica Microsystems GmbH; magnification, x200 and x400.

Cell culture and transfection. NRK-52E cells (Kunming Cell Bank, Chinese Academy of Sciences) were cultured in Dulbecco's modified Eagle's medium (HyClone; Cytiva) supplemented with 5% fetal bovine serum (Gibco; Thermo Fisher Scientific, Inc.) and 5.5 mmol/l glucose in 25-cm^2 culture flasks in an incubator with 5% CO_2 at 37˚C. Prior to changing to a serum-free medium for 20 h to maintain the pace of growth or following transfection, the cells were treated with the following media: i) Normal glucose (NG group, 5.5 mmol/l glucose, cultured for 48 h; ii) high-glucose control (HG) group, 5.5 mmol/l glucose +19.5 mmol/l D-glucose, cultured for 48 h; iii) high glucose to normal glucose (HG to NG) group, cultured under high-glucose medium for 24 h and then transferred to normal glucose medium for another 24 h. Transient transfection of NRK-52E cells was performed using Lipofectamine® 3000 (Invitrogen; Thermo Fisher Scientific, Inc.) according to the manufacturer's instructions. Transfection was started when 50-60% of cells were fused. DMEM culture medium, 6 μl Lipofectamine® 3000 and 3 μg Skil shRNA plasmid were mixed and placed in a sterile environment for 20 min. After the transfection reagent was added to the cells and cultured for 6 h (37˚C), the culture medium was replaced. Following 48 h culturing (37˚C) in high-glucose medium, the cells were collected for western blotting to detect the corresponding protein expression levels (SnoN, E-cadherin, α-SMA). The Skil shRNA (Sh Skil) plasmid was manufactured by Guangzhou RiboBio Co., Ltd., and the sequences were as follows: Sh Skil sense, 5'-CCGGGATTCATCGGTCTCAAATAATCTCGAGATTATTTGAGACCGATGAATCTTTTTG-3' and antisense, 5'-AATTCAAAAAGATTCATCGGTCTCAAATAATCTCGAGATTATTTGAGACCGATGAATC-3'; and scrambled control shRNA sense, 5'-CCGGCAACAAGATGAAGAGCACCAACTCGAGTTGGTGCTCTTCATCTTGTTGTTTTTG-3' and antisense, 5'-AATTCAAAAACAACAAGATGAAGAGCACCAACTCGAGTTGGTGCTCTTCATCTTGTTG-3'.

Western blotting. Renal tissue samples were homogenized in lysis buffer (Beyotime Institute of Biotechnology). After grinding for 2 min in a high-speed automatic grinding machine, the supernatant was centrifuged at 4˚C (16,502 x g, 15 min) and the protein concentration of each sample was detected by BCA kit. Proteins were separated by 10% SDS-PAGE, then PVDF membrane was transferred and sealed, using 50 g/l skimmed milk at room temperature for 1 h. Rabbit TGF-β1 (1:500; Santa Cruz Biotechnology, Inc.; cat sc-130348), SnoN (1:1,000; Abcam; cat ab58846), Smurf2 (1:1,000; Cell Signaling Technology, Inc.; cat 12024s), mouse Arkadia (1:500; Santa Cruz Biotechnology, Inc.; cat sc-134270), rabbit E-cadherin (1:1,000; ProteinTech Group, Inc.; cat 20874-1-AP), α-SMA (1:1,000; ProteinTech Group, Inc.; cat 14395-1-AP), phospho(p)-Smad2 (1:1,000; Cell Signaling Technology, Inc.; cat 18338S), Smad2 (1:500; Santa Cruz Biotechnology, Inc.; cat sc-101153), p-Smad3 (1:1,000; Cell Signaling Technology, Inc.; cat 9520S), Smad3 (1:1,000; Abcam; cat ab40854) and β-actin (1:4,000; cat. no. PMK083S; Wuhan Pomeike Biotechnology Co., Ltd.) antibodies were added and incubated overnight at 4˚C. After washing three times with TBST, corresponding horseradish peroxidase-labeled secondary IgG (1:8,000; BioPM; cat. no. PMK083S) was added and incubated at room temperature for 1 h. After washing three times with TBST, proteins were detected using an enhanced

chemiluminescence system (Tanon-5200; Tanon Science and Technology Co., Ltd.) and ECL Hyperfilm (Smart Life Sciences, Ltd.; cat. no. H31500).

RNA extraction and RT-qPCR. Total RNA was extracted from renal tissues using an RNA extraction kit (Tiangen Biotech Co., Ltd.) and reverse-transcribed (30 cycles of 94˚C for 45 sec, 60˚C for 45 sec and 72˚C for 2 min, followed by final extension for 7 min at 72˚C) using a Takara RNA PCR kit (Takara Biotechnology Co., Ltd.; cat RR037A). The cDNA was amplified in a gradient thermal cycler (initial denaturation at 95˚C for 30 sec, followed by 40 cycles of 95˚C for 5 sec and 60˚C for 30-34 sec) (Bio-Rad Laboratories, Inc.) using a SYBR® Green Supermix (Bio-Rad Laboratories, Inc.). The Cq values and relative expression levels between SnoN and β-actin were calculated using the $2^{-\Delta\Delta Cq}$ method (19). The primer sequences were as follows: SnoN forward, 5'-GTCTGGAGTGTTGTGG AATGTTT-3' and reverse, 5'-TTCAGTTTCTTTTCTTCAGG TGT-3' (163 bp); and β-actin forward, 5'-GCCAACACAGTG CTGTCT-3' and reverse, 5'-AGGAGCAATGATCTTGAT CTT-3' (114 bp).

Immunoprecipitation. Immunoprecipitation was performed using an Immunoprecipitation kit Dynabeads® Protein G (Thermo Fisher Scientific, Inc.; cat. no. 88804) according to the manufacturer's instructions. Renal tissue samples were homogenized in lysis buffer (500 μl; Beyotime Institute of Biotechnology) and the proteins were incubated with agarose beads (20-100 μl) coupled with SnoN antibody (1:1,000; Abcam; cat ab58846). To remove non-specific binding, samples were mixed and washed with Wash Buffer and gently vortexed to mix. The tube was placed into a magnetic stand to collect the beads and the supernatant was discarded. Then, 1 ml IP Lysis/Wash Buffer was added to the tube and gently vortexed for 1 min. Beads were collected with the magnetic stand and supernatant was discarded. This process was repeated three times. Immunoprecipitated proteins were eluted by adding 50 μl Elution Buffer to the tube at room temperature for 10 min. Beads were magnetically separated and supernatant containing the target antigen was collected. To neutralize the low pH, 5 μl Neutralization Buffer/50 μl eluate was added. The SnoN ubiquitylation was determined by incubation with rabbit ubiquitin (UB) antibody (4˚C overnight; 1:100; Abcam; cat. no. ab140601).

Malonaldehyde (MDA) and catalase (CAT) assays. A total of 0.02 g renal tissue was weighed and normal saline was added in a body weight:volume of 1:9. The 10% homogenate was made by homogenizer (cat. no. SCIENTZ-48; Ningbo Scientz Biotechnology Co., Ltd.), and the supernatant was centrifuged at 4˚C (16,502 x g; 15 min). MDA content and CAT activity were assessed using commercial kits (cat. nos. A003-1-2 and A007-1-1, respectively; both Nanjing Jiancheng Bioengineering Research Institute) according to the manufacturer's instructions.

Statistical analysis. Each experiment was repeated at least twice. Data are presented as the mean ± SD. Statistical analysis was performed using the SPSS 23.0 (IBM Corp.) and GraphPad Prism 8.0.2 (GraphPad Software, Inc.) software. Differences were analyzed using one-way analysis of variance (ANOVA) followed by the least significant difference post hoc test for multiple comparisons. $P<0.05$ was considered to indicate a statistically significant difference.

Results

Insulin treatment reverses STZ-induced changes in diabetes-associated parameters. Fasting blood glucose (Fig. 1A), HbA1c (Fig. 1B), 24-h urine protein (Fig. 1C) and malondialdehyde (MDA; Fig. 1F) levels were increased in the DM group compared with those in the NC group (all $P<0.05$), whereas the body weight (Fig. 1D) and catalase (CAT) activity (Fig. 1E) were significantly decreased (both $P<0.05$). Compared with DM group, insulin group exhibited a decrease in fasting blood glucose, HbA1c, 24-h urine protein and MDA levels, whereas the body weight and CAT levels were increased compared with those in the DM group ($P<0.05$). These results suggested that the diabetic rat model was successfully established using STZ and that insulin affected the STZ-induced changes in blood glucose and body weight. The increases in the 24-h urine protein levels in the DM group compared with those in the NC group indicated the development of DN.

To analyze the therapeutic effects of insulin on the kidney, renal pathology was examined with H&E and Masson staining (Fig. 1G). Pathological changes in the kidneys of rats in the DM were observed; the glomerular volume and tubulointerstitial area increased, and the tubulointerstitial area of the DM group appeared larger compared with that of the NC group. Collagen serves a critical structural role in the renal fibrosis of DN (20). The results of light microscopy following Masson staining revealed that the extent of Col-III accumulation in the kidneys of the DM group appeared to be higher compared with that in the NC group; this effect was decreased by insulin treatment.

Insulin reverses HG-induced EMT and ECM accumulation. Consistent with the results of Masson staining, western blotting data suggested that the levels of p-Smad2 (Ser465/467) and p-Smad3 (Ser423/425) in the DM group were higher compared with those in the NC group ($P<0.05$; Fig. 2A and B). Compared with those in the DM group, the levels of p-Smad2 and p-Smad3 were significantly decreased in the INS group ($P<0.05$). Excessive ECM deposits in the kidneys are a hallmark of tubulointerstitial fibrosis. High expression levels of TGF-β1 directly induce the deposition of ECM under HG conditions and stimulate renal tubular epithelial cells to differentiate into myofibroblasts, which leads to excessive deposition of ECM and the development of tubulointerstitial fibrosis (21). Therefore, the present study further assessed the effects of insulin treatment on Col-III, E-cadherin and α-SMA expression levels in the renal tissues of DM rats. The levels of TGF-β1, collagen III and α-SMA significantly increased, whereas the protein levels of E-cadherin decreased in the DM group compared with those in the NC group ($P<0.05$; Fig. 2C and D). Following insulin treatment, the expression levels of TGF-β1, Col-III and α-SMA decreased, and the levels of E-cadherin protein increased compared with those in the DM group (Fig. 2C and D). In addition, immunofluorescence

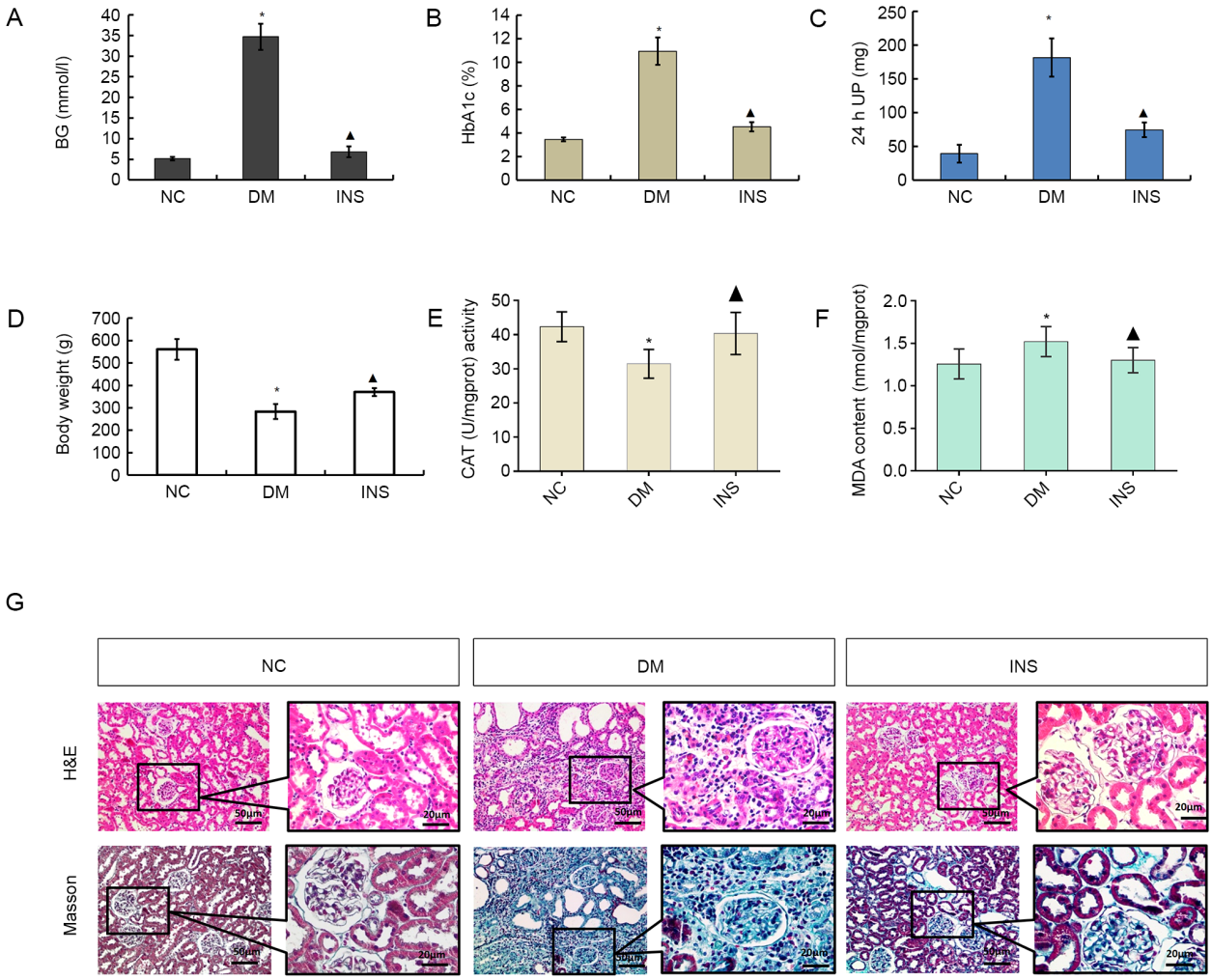

Figure 1. STZ-induced changes in (A) BG, (B) HbA1c, (C) 24 h UP, (D) body weight, (E) CAT and (F) MDA levels. n=8. *P<0.05 vs. NC; ▲P<0.05 vs. DM. (G) Histological changes in kidneys in each group. Magnification, x200 and x400. Black box indicates the enlarged area of fibrosis. STZ, streptozotocin; HbA1c, glycosylated hemoglobin A1; 24 h UP, 24-h urine protein; CAT, catalase; MDA, malondialdehyde; NC, normal control; DM, diabetes mellitus; INS, insulin.

analysis revealed that E-cadherin was mainly expressed in the renal tubular epithelial membrane in the NC group, which was decreased in the DM group; compared with that in the DM group, E-cadherin expression in the INS group was restored (Fig. 2E). Immunohistochemical staining demonstrated that the expression of Col-III in the DM group was increased compared with that in the NC group, and this effect was reversed by insulin treatment (Fig. 2F).

Insulin partially attenuates HG-induced downregulation of SnoN. Renal tissue western blotting demonstrated that the protein expression levels of SnoN were reduced in the DM group compared with those in the NC group (P<0.05; Fig. 3A and B). The protein levels of SnoN in renal tissues of rats in the NC and DM groups were detected by immunoprecipitation, and western blotting was performed with a UB antibody. The results demonstrated that STZ-induced DM increased the levels of ubiquitylation and degradation of SnoN (Fig. 3D); however, compared with those in the DM group, the ubiquitin levels and degradation of SnoN in the INS group were partially reversed by insulin (P<0.05). In addition, RT-qPCR results demonstrated that the mRNA levels of SnoN were increased in the DM group compared with those in the NS group (P<0.05), whereas the INS group presented with levels similar to those in the NC group (Fig. 3C).

E3 ubiquitin enzymes Smurf2 and Arkadia were weakly expressed in the NC group, but highly expressed in the DM group (P<0.05; Fig. 3A and B), which suggested that DM induced the activation of the ubiquitin-proteasome pathway. However, the DM-elevated Smurf2 and Arkadia expression levels in rat renal tissues were significantly decreased by insulin and were similar to those observed in the NC group.

To determine whether insulin-dependent control of blood glucose levels slowed down the fibrotic changes of tubular cells via SnoN, an *in vitro* model was established by culturing NRK-52E cells in HG medium for 24 h, followed by NG for 24 h. The results demonstrated that the return to NG recovered the protein expression levels of SnoN and intervened EMT (E-Ca protein increased and α-SMA protein decreased) compared with those observed in the HG group. This trend was diminished by transfection of the Sh Skil plasmid into NRK-52E cells, which the level of SnoN protein decreased and promoted EMT (P<0.05; Fig. 3E and F).

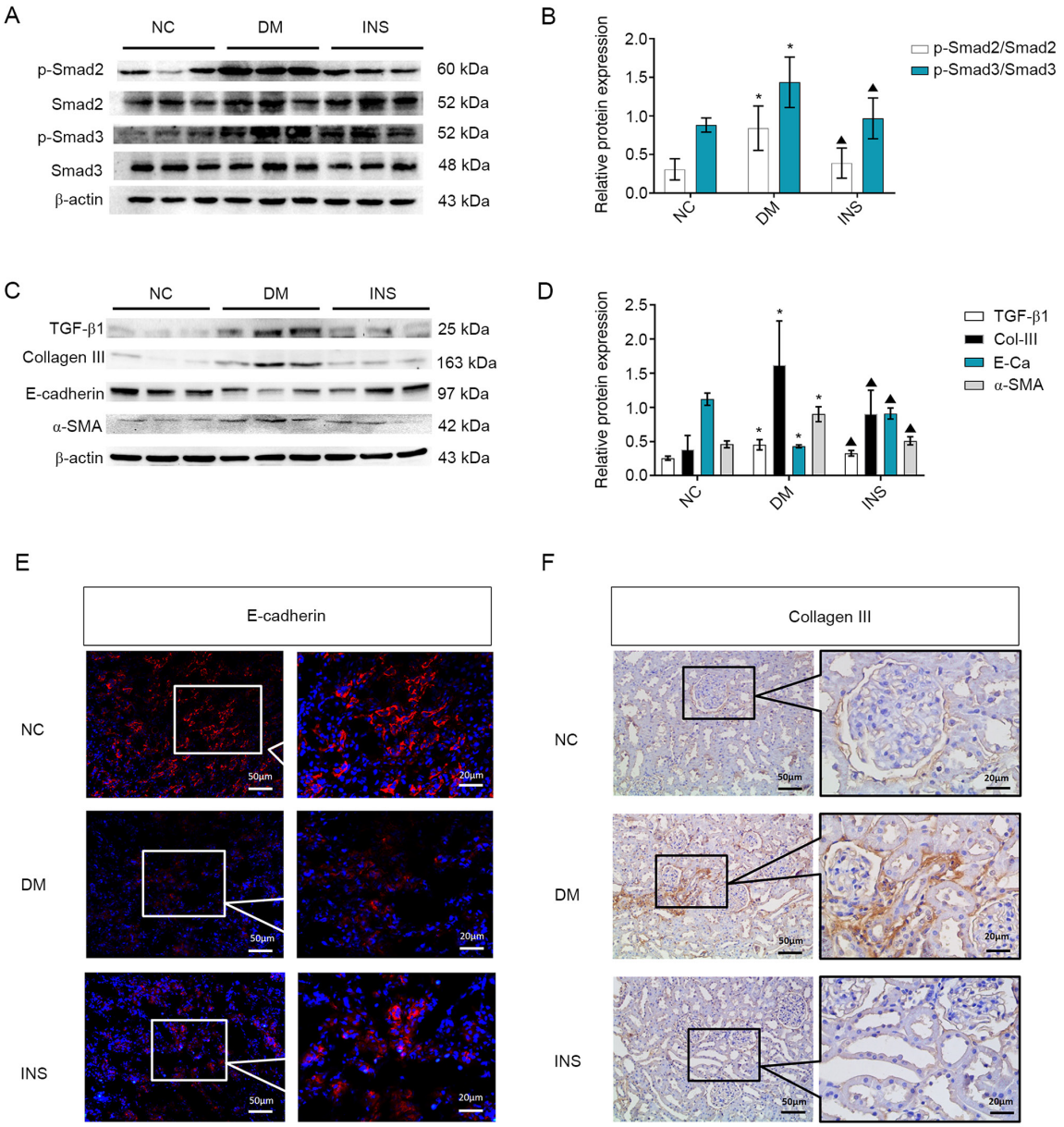

Figure 2. Activation of TGF-β1, EMT and ECM accumulation. (A) Representative western blots and (B) quantitative analysis of the levels of p-Smad2, Smad2, p-Smad3 and Smad3 in the kidney tissues of rats from different groups. (C) Representative western blots and (D) quantitative analysis of the expression levels of TGF-β1, Col-III, E-cadherin and α-SMA in the kidney tissues in the three groups. n=8. *P<0.05 vs. NC; ▲P<0.05 vs. DM. (E) Immunofluorescence staining of E-cadherin. (F) Immunohistochemical staining of Col-III in the kidney tissues of rats in the three groups. Black box indicates the enlarged. TGF-β1, transforming growth factor β1; EMT, epithelial-mesenchymal transition; ECM, extracellular matrix; p, phosphorylated; Col, collagen; α-SMA, α-smooth muscle actin; NC, normal control; DM, diabetes mellitus; INS, insulin.

Discussion

Previous studies have demonstrated that the expression of TGF-β1 is enhanced during the pathogenesis of renal fibrosis (22,23). TGF-β1 serves an important role in promoting fibrosis and functions as a cytokine involved in the incidence and development of renal fibrosis-related disease (6,9). For example, TGF-β1 exerts its profibrotic activity via stimulation of fibroblast proliferation, extracellular matrix protein synthesis (such as collagen I, III and IV, proteoglycans, laminin and fibronectin), and EMT (22). Therefore, preventing TGF-β1-induced fibrosis may aid renal fibrosis prevention and treatment. SnoN is a negative regulator of the TGF-β1/Smads signaling pathway that directly interacts with the Smads protein (24). In the cytoplasm, SnoN inhibits Smad2/3-Smad4 complex formation and nuclear translocation, whereas in the nucleus, it interferes with activated Smads and initiates the transcription of various TGF-β1 target genes (such as collagen I, III and IV) (7,25).

Previous studies have assessed the expression and effects of SnoN during DN pathogenesis and reported that SnoN expression levels decrease during DN progression, which is accompanied by ECM deposits in the renal interstitium and the occurrence of the EMT (9,11). Notably, SnoN inhibition in tubular epithelial cells by small interfering RNA further upregulates HG-induced fibronectin and α-SMA expression, which aggravates fibrotic lesions (8). In the present study, SnoN mRNA and TGF-β1 protein levels in renal tissues of

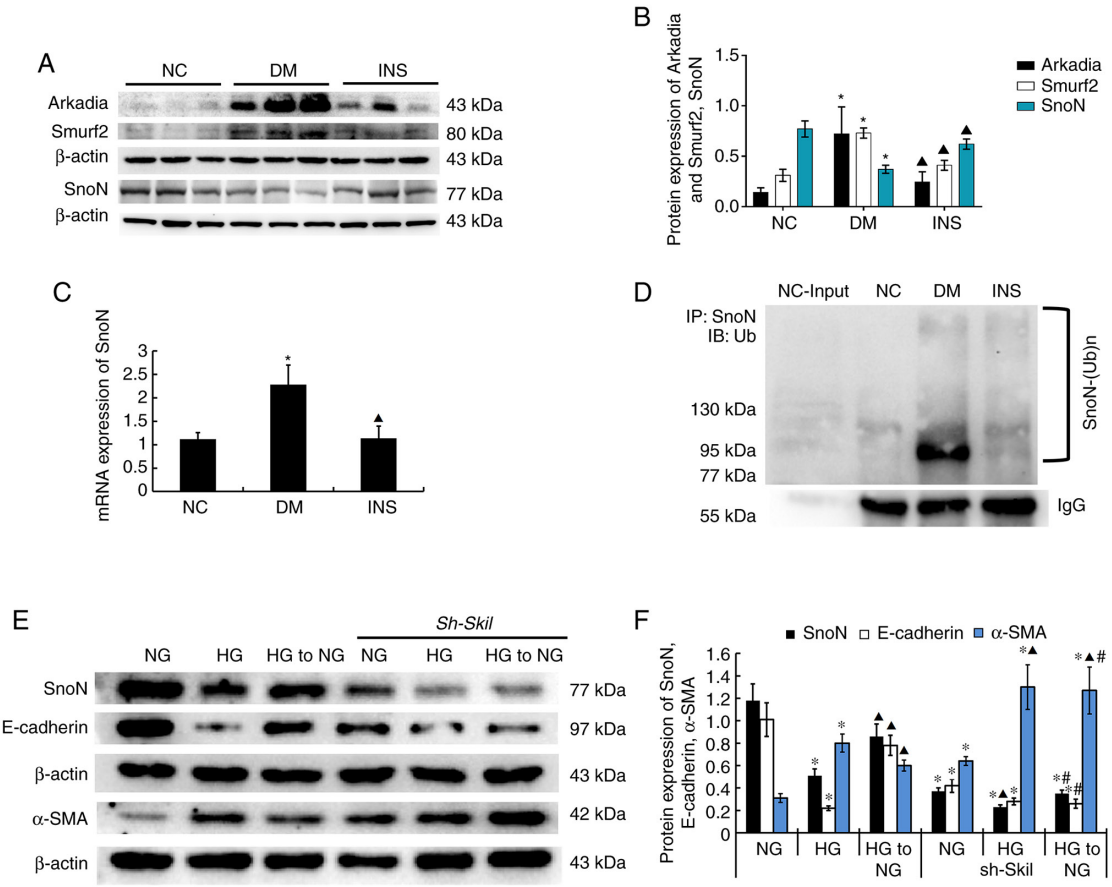

Figure 3. SnoN distribution and expression in kidney tissue specimens. (A) Representative western blot and (B) quantitative data of the expression levels of Arkadia, Smurf2 and SnoN in the kidney tissues in different groups. (C) SnoN mRNA expression levels in the kidney tissues of rats in different groups. n=8. *P<0.05 vs. NC; ▲P<0.05 vs. DM. (D) Ubiquitylation of SnoN in the kidney tissues in different groups. Representative (E) western blot and (F) quantitative data are revealed the expression of SnoN, E-cadherin, α-SMA in NRK-52E cells under different conditions. n=3. *P<0.05 vs. NG; ▲P<0.05 vs. HG; #P<0.05 vs. HG to NG. SnoN, Ski-related novel protein N; Smurf2, Smad ubiquitin regulatory factor 2; NC, normal control; DM, diabetes mellitus; INS, insulin; NG, normal glucose; HG, high glucose; Sh Skil, short hairpin RNA targeting SnoN; IP, immunoprecipitation; IB, immunoblot; Ub, ubiquitin.

diabetic rats were inhibited and upregulated, respectively, compared with those in the NC rats. In addition, inconsistent results were obtained in the DM group for SnoN mRNA and protein levels: The SnoN mRNA expression levels were higher in the DM group compared with those in the control group. TGF-β1 stimulation for 2 h has been reported to promote the transcriptional activation of SnoN in cancer cells in a negative feedback mechanism that limits the TGF-β1/Smads signal transduction (5,11,26). However, our and other studies have demonstrated that TGF-β1 can rapidly and significantly decrease the levels of the SnoN protein by activating TAK1 (15,16), which phosphorylates SnoN and affects its stability (15). Subsequently, p-SnoN is downregulated by E3 ubiquitin enzyme-mediated degradation involving Smurf2 and Arkadia (13,14). E3 ubiquitin ligase, ubiquitin-activating enzyme (E1) and ubiquitin-conjugating enzyme (E2) are the components of the ubiquitin proteasome system (UPS), which mediates protein degradation via a cascade of responses (27). E3 ubiquitin ligase serves a decisive role in the UPS by determining the selectivity and specificity of substrate proteins (28), whereas Smurf2 and Arkadia are specific regulators that mediate the UPS to regulate the degradation of SnoN protein (14,28). As aforementioned, Smurf2 and Arkadia were highly expressed in the renal tissues of DN rats in the present study. TGF-β enhances its biological effects by modulating the Arkadia-mediated SnoN degradation (29,30). Arkadia binds the SnoN protein with the carboxy-terminal RING domain (28) and induces ubiquitin-mediated degradation of the SnoN protein in the presence of p-Smad2/3 involvement (31). Following activation by TGF-β1, Smad2/3 mediates the interaction between Smurf2, Arkadia and SnoN, which allows the homologous E6-APC-terminus of Smurf2 and Arkadia to target SnoN, inducing the ubiquitin degradation of the SnoN protein (14,30,32). Therefore, although the TGF-β1/Smads signaling pathway upregulates SnoN expression at the transcriptional level, it is not sufficient to offset or reverse the ubiquitin-mediated degradation of SnoN induced by Smurf2 and Arkadia through this pathway, which causes decreased SnoN protein levels in DN rats and alters the negative feedback inhibition effect of the TGF-β1/Smads signaling pathway, inducing fibrotic lesions in DN.

HG is the initial factor promoting the decrease of SnoN protein level in renal tubular epithelial cells, and blood glucose control by insulin can prevent and delay the development of DN (17,18). In addition, HG also induces oxidative stress and aggravates the development of DN. In the present study, the metabolic function of rats significantly improved and renal fibrotic lesions were alleviated by insulin treatment compared

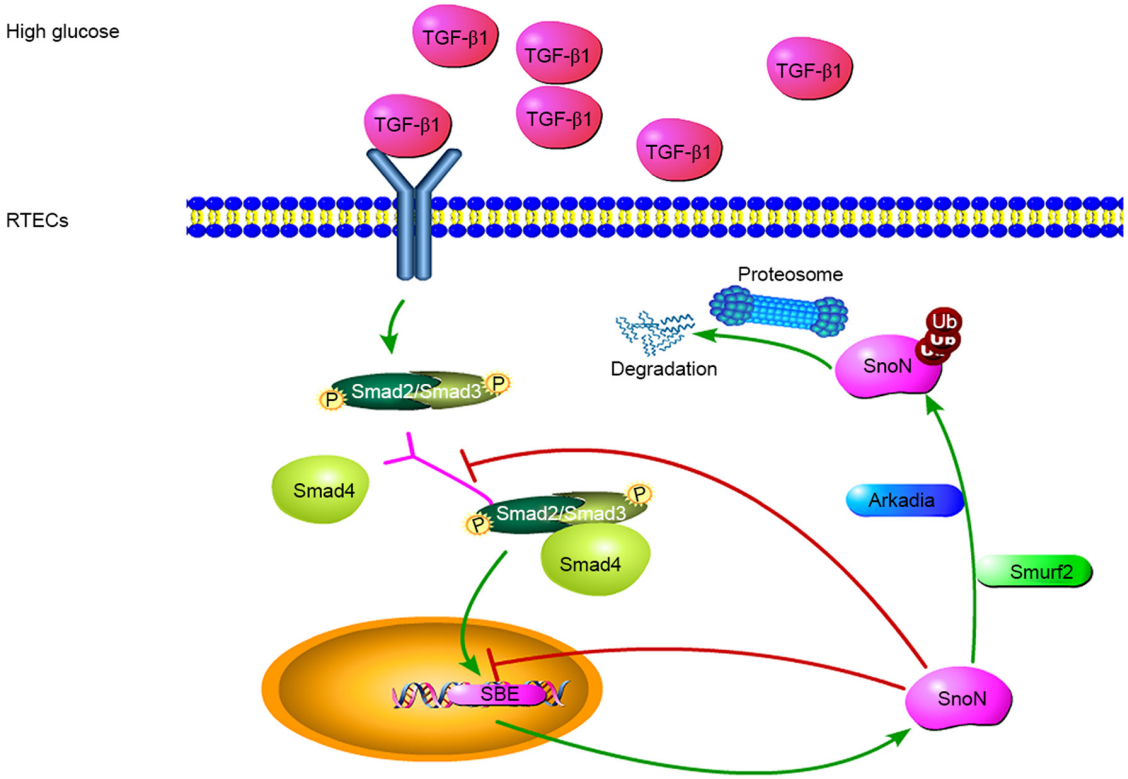

Figure 4. Potential mechanisms of TGF-β1/Smads-dependent regulation of SnoN during DN. TGF-β1 is involved in the regulation of fibrosis, and TGF-β1/Smads is the canonical pathway for its biological functions. In a high-glucose environment, cells secrete TGF-β1, leading to the phosphorylation of Smads, which form a complex to regulate the expression of SnoN. During the occurrence and development of DN, the level of SnoN protein may be reduced through UPS-mediated degradation of SnoN protein, reversing the transcriptional activation of SnoN. TGF-β1 mediates E3 ubiquitin ligase and induces SnoN protein degradation. Thus, the amount of SnoN protein in renal tubular epithelial cells depends on the balance between these two effects. Both processes are mediated by the TGF-β1/Smads/SnoN signaling pathway, which leads to the fibrosis amplification, promoting the occurrence and development of DN. TGF-β1, transforming growth factor β1; SnoN, Ski-related novel protein N; Smurf2, Smad ubiquitin regulatory factor 2; Ub, ubiquitin; p, –phosphorylation; UPS, ubiquitin proteasome system; SBE, Smads binding element.

with those in the DM group. The decreased blood glucose and glycated hemoglobin levels indicated that hyperglycemia was improved. Additionally, the expression levels of Smurf2 and Arkadia significantly decreased following insulin treatment. The expression of SnoN was lower at the transcriptional level, but was enhanced at the protein level in the INS group compared with the DM group. In addition, the phenotypes of renal tubular epithelial cells and ECM deposits appeared to be reduced following insulin treatment compared with those in the DM group. Therefore, the control of blood glucose may delay the development of DN and improve the stability of SnoN protein.

The results of the present study demonstrated that a dual mechanism contributed to the regulation of SnoN by TGF-β1 *in vivo* by comparing and analyzing data obtained before and after blood glucose control in DM rats. On the one hand, TGF-β1 induced SnoN expression; on the other hand, TGF-β1 mediated E3 ubiquitin ligase-induced SnoN protein degradation. Therefore, the SnoN protein amounts in renal tubular epithelial cells may depend on the balance between these two effects (Fig. 4).

In conclusion, decreased expression of SnoN protein was observed due to the combined effect of promoting transcriptional activation of SnoN and mediating ubiquitination degradation of SnoN protein by Arkadia and Smurf2 following activation of the TGF-β/Smads signaling pathway in the pathogenesis of DN. Blood glucose control delayed the progression of DN by restoring SnoN protein levels.

Acknowledgements

Not applicable.

Funding

This work was supported by the Regional Common Diseases and Adult Stem Cell Transformation Research and Innovation Platform of Guizhou Provincial Department of Science and Technology [grant no. (2019) 4008], the Guizhou province Science and Technology Funding [grant no. QianKeHeBase (2017) 5718] and the Guiyang Science and Technology Funding [grant no. ZhuKe (2017) 30-20].

Availability of data and materials

The datasets used and/or analyzed during the current study are available from the corresponding author on reasonable request.

Authors' contributions

LQL designed and performed additional experiments, analyzed the data, wrote, revised and finalized the manuscript. SL and

YWM performed the animal experiments. SL analyzed the data and revised the manuscript. LLL, HML, XHZ, WP and YX performed the experiments. FZ analyzed the data and revised the manuscript. MJS participated in the drafting of the manuscript and data interpretation. YYW participated in data interpretation and critically revised the contents. BG conceived and designed the study. All authors read and approved the final manuscript. LQL, YYW and BG confirm the authenticity of all the raw data.

Ethics approval and consent to participate

The study was conducted in accordance with the guidelines of the National Health and Medical Research Council of China's code for the care and use of animals for scientific purposes and was approved by the Animal Experimental Ethical Inspection Form of Guizhou Medical University (approval no. 1503092).

Patient consent for publication

Not applicable.

Competing interests

The authors declare that they have no competing interests.

References

1. Flyvbjerg A: The role of the complement system in diabetic nephropathy. Nat Rev Nephrol 13: 311-318, 2017.
2. Gu W, Liu Y, Chen Y, Deng W, Ran X, Chen L, Zhu D, Yang J, Shin J, Lee SW, *et al*: Multicentre randomized controlled trial with sensor-augmented pump vs multiple daily injections in hospitalized patients with type 2 diabetes in China: Time to reach target glucose. Diabetes Metab 43: 359-363, 2017.
3. Valencia WM and Florez H: How to prevent the microvascular complications of type 2 diabetes beyond glucose control. BMJ 356: i6505, 2017.
4. Xiong Y and Zhou L: The Signaling of Cellular Senescence in Diabetic Nephropathy. Oxid Med Cell Longev 2019: 7495629, 2019.
5. Li J, Wu B, Hu H, Fang X, Liu Z and Wu S: GdCl3 attenuates the glomerular sclerosis of streptozotocin (STZ) induced diabetic rats via inhibiting TGF-β/Smads signal pathway. J Pharmacol Sci 142: 41-49, 2020.
6. Sutariya B, Jhonsa D and Saraf MN: TGF-β: The connecting link between nephropathy and fibrosis. Immunopharmacol Immunotoxicol 38: 39-49, 2016.
7. Zeglinski MR, Hnatowich M, Jassal DS and Dixon IM: SnoN as a novel negative regulator of TGF-β/Smad signaling: A target for tailoring organ fibrosis. Am J Physiol Heart Circ Physiol 308: H75-H82, 2015.
8. Liu R, Wang Y, Xiao Y, Shi M, Zhang G and Guo B: SnoN as a key regulator of the high glucose-induced epithelial-mesenchymal transition in cells of the proximal tubule. Kidney Blood Press Res 35: 517-528, 2012.
9. Liu L, Wang Y, Yan R, Li S, Shi M, Xiao Y and Guo B: Oxymatrine Inhibits Renal Tubular EMT Induced by High Glucose via Upregulation of SnoN and Inhibition of TGF-β1/Smad Signaling Pathway. PLoS One 11: e0151986, 2016.
10. Luo DD, Phillips A and Fraser D: Bone morphogenetic protein-7 inhibits proximal tubular epithelial cell Smad3 signaling via increased SnoN expression. Am J Pathol 176: 1139-1147, 2010.
11. Jahchan NS and Luo K: SnoN in mammalian development, function and diseases. Curr Opin Pharmacol 10: 670-675, 2010.
12. Liu S, Yu N, Zhang XL, Chen XQ and Tang LQ: Regulatory effect of berberine on unbalanced expressions of renal tissue TGF-beta1/SnoN and smad signaling pathway in rats with early diabetic nephropathy. Zhongguo Zhongyao Zazhi 37: 3604-3610, 2012 (In Chinese).
13. Sakairi T, Hiromura K, Takahashi S, Hamatani H, Takeuchi S, Tomioka M, Maeshima A, Kuroiwa T and Nojima Y: Effects of proteasome inhibitors on rat renal fibrosis in vitro and in vivo. Nephrology (Carlton) 16: 76-86, 2011.
14. Wang Y, Zhang X, Mao Y, Liang L, Liu L, Peng W, Liu H, Xiao Y, Zhang Y, Zhang F, *et al*: Smad2 and Smad3 play antagonistic roles in high glucose-induced renal tubular fibrosis via the regulation of SnoN. Exp Mol Pathol 113: 104375, 2020.
15. Wang Y, Mao Y, Zhang X, Liu H, Peng W, Liang L, Shi M, Xiao Y, Zhang Y, Zhang F, *et al*: TAK1 may promote the development of diabetic nephropathy by reducing the stability of SnoN protein. Life Sci 228: 1-10, 2019.
16. Kajino T, Omori E, Ishii S, Matsumoto K and Ninomiya-Tsuji J: TAK1 MAPK kinase kinase mediates transforming growth factor-beta signaling by targeting SnoN oncoprotein for degradation. J Biol Chem 282: 9475-9481, 2007.
17. Satirapoj B and Adler SG: Prevalence and Management of Diabetic Nephropathy in Western Countries. Kidney Dis 1: 61-70, 2015.
18. Zhang Q, Li Y and Chen L: Effect of berberine in treating type 2 diabetes mellitus and complications and its relevant mechanisms. Zhongguo Zhongyao Zazhi 40: 1660-1665, 2015 (In Chinese).
19. Livak KJ and Schmittgen TD: Analysis of relative gene expression data using real-time quantitative PCR and the 2(-Delta Delta C(T)) Method. Methods 25: 402-408, 2001.
20. Mise K, Ueno T, Hoshino J, Hazue R, Sumida K, Yamanouchi M, Hayami N, Suwabe T, Hiramatsu R, Hasegawa E, *et al*: Nodular lesions in diabetic nephropathy: Collagen staining and renal prognosis. Diabetes Res Clin Pract 127: 187-197, 2017.
21. Kato M, Park JT and Natarajan R: MicroRNAs and the glomerulus. Exp Cell Res 318: 993-1000, 2012.
22. Loboda A, Sobczak M, Jozkowicz A and Dulak J: TGF-β1/Smads and miR-21 in Renal Fibrosis and Inflammation. Mediators Inflamm 2016: 8319283, 2016.
23. Sun Z, Ma Y, Chen F, Wang S, Chen B and Shi J: miR-133b and miR-199b knockdown attenuate TGF-β1-induced epithelial to mesenchymal transition and renal fibrosis by targeting SIRT1 in diabetic nephropathy. Eur J Pharmacol 837: 96-104, 2018.
24. Deheuninck J and Luo K: Ski and SnoN, potent negative regulators of TGF-β signaling. Cell Res 19: 47-57, 2009.
25. Ma T-T and Meng XM: TGF-β/Smad and Renal Fibrosis. Adv Exp Med Biol 1165: 347-364, 2019.
26. Stroschein SL, Wang W, Zhou S, Zhou Q and Luo K: Negative feedback regulation of TGF-beta signaling by the SnoN oncoprotein. Science 286: 771-774, 1999.
27. Ciechanover A, Orian A and Schwartz AL: The ubiquitin-mediated proteolytic pathway: Mode of action and clinical implications. J Cell Biochem Suppl 34: 40-51, 2000.
28. Inoue Y and Imamura T: Regulation of TGF-beta family signaling by E3 ubiquitin ligases. Cancer Sci 99: 2107-2112, 2008.
29. Li XZ, Feng JT, Hu CP, Chen ZQ, Gu QH and Nie HP: Effects of Arkadia on airway remodeling through enhancing TGF-beta signaling in allergic rats. Lab Invest 90: 997-1003, 2010.
30. Briones-Orta MA, Levy L, Madsen CD, Das D, Erker Y, Sahai E and Hill CS: Arkadia regulates tumor metastasis by modulation of the TGF-β pathway. Cancer Res 73: 1800-1810, 2013.
31. Levy L, Howell M, Das D, Harkin S, Episkopou V and Hill CS: Arkadia activates Smad3/Smad4-dependent transcription by triggering signal-induced SnoN degradation. Mol Cell Biol 27: 6068-6083, 2007.
32. Tan R, He W, Lin X, Kiss LP and Liu Y: Smad ubiquitination regulatory factor-2 in the fibrotic kidney: Regulation, target specificity, and functional implication. Am J Physiol Renal Physiol 294: F1076-F1083, 2008.